

Effect of Ni concentration on the structural and hydrogen storage characteristics of Zr–Mn based laves phase system

Vinod Kumar · D. Pukazhselvan · A. K. Tyagi · S. K. Singh

Received: 4 December 2012 / Accepted: 21 March 2013 / Published online: 3 April 2013
© The Author(s) 2013. This article is published with open access at Springerlink.com

Abstract The present communication reports the hydrogen storage characteristics of $\text{ZrMn}_{2-x}\text{Ni}_x$ laves phase hydrides. It is observed that promising hydrogen storage materials can be tailored when “ x ” is in the range of $1.5 \leq x \leq 1$. The materials formed within this range reversibly store ~ 2 to ~ 3 H/F.U. under manageable operating conditions. The composition $\text{ZrMn}_{0.5}\text{Ni}_{1.5}$ is found to absorb and desorb hydrogen under room temperature. The other two compositions $\text{ZrMn}_{0.75}\text{Ni}_{1.25}$ and ZrMnNi absorb ~ 3.6 H/F.U. and release ~ 3 and ~ 3.2 H/F.U., respectively. In each case, almost half of the effective storage capacity of total can be reversibly stored within 5 s under room temperature. Therefore, the materials falling within the range of $1.5 \leq x \leq 1$ are promising candidates for stationary device applications. The correlation between the compositions, structural–microstructural features and thermodynamic data are presented.

Keywords Laves phase · Hydrogen storage · Crystal structure · Thermodynamics

Introduction

ZrMn_2 laves phase alloy attracts much attention due to its higher storage capacity (~ 1.7 wt%) with rapid H absorption kinetics [1]. However, hydrogen desorption occurs only at elevated temperatures which restricts its application potential for variety of devices such as heat pumps, Ni/MH batteries, stationary hydrogen storage cylinders, etc. Researchers have shown that the desorption characteristics of ZrMn_2 system can be improved by doping/alloying with suitable metals [2–5]. The work of Matsumura et al. [6] revealed that the reason for the higher stability of the ZrMn_2 hydride is due to the higher bond strength between the stored H with Mn atoms. They have also shown that the bond strengths between Zr–Mn, Mn–Mn and Mn–H all get significantly modified by doping by other suitable metals. Both the Zr and Mn sites can be substituted with hyper/hypo-stoichiometry of the laves phase which often makes the presence of substitute atoms even in excess of 10 per formula unit [7–13]. It may be pointed out that incorporation of several metal atoms results in unwanted side reaction [14]. As for example, dissolution of constituent metal atoms of MH electrode in the electrolyte of an electrochemical device costs its durability.

In an earliest study, Suzuki and Nishimiya [15] have investigated hydrogen storage characteristics of $\text{ZrMn}_{1.6}\text{Ni}_{0.4}$, ZrMnNi and $\text{ZrMn}_{0.4}\text{Ni}_{1.6}$ systems and shown that the dissociation pressure of the ZrMn_2 system gets significantly enhanced with the incorporation of Ni content. They have also concluded that ZrMnNi is the most promising hydride with the hydrogen filling of ~ 3.5 hydrogen atoms per formula unit under near ambient conditions. Kim et al. [16] have studied several Zr–Mn–Ni–V alloys and observed that the equilibrium plateau pressure gets significantly enhanced with the concentration of Ni content.

V. Kumar · D. Pukazhselvan · S. K. Singh (✉)
Hydrogen Energy Lab, Department of Physics, Deenbandhu
Chhotu Ram University of Science and Technology,
Murthal (Sonapat), Haryana, India
e-mail: sksingh2k6@gmail.com

D. Pukazhselvan
Department of Physics and Astronomy, Padova University,
Padua, Italy

A. K. Tyagi
Solid State Chemistry Section, Babha Atomic Research Centre,
Trombay, Mumbai, India

However, there was significant reduction in the hydrogen capacity and the rate of reaction. The authors attributed the effect to the amount of reactive surfaces, since the presence of more Ni limits the amount of reactive surfaces while offering excellent catalytic activity. We have studied a series of Zr based systems, namely $\text{ZrMn}_{2-x}\text{Ni}_x$, where $x = 0$ to 2. XRD analysis revealed that the Mn rich compositions possess C14 hcp structure, whereas the Ni rich compositions exhibit C15 cubic structure. Hence, at a particular concentration of Zr–Mn–Ni the C14 structure transforms to C15 structure. We observed that except ZrNi_2 all the other composition studied in the present investigation absorbs above 3 H/F.U. under room temperature. The dehydrogenation from ZrMn_2 is found to be possible only above 250 °C, but Mn–Ni coexisting system exhibits very interesting desorption characteristics. Particularly, we observed that $\text{ZrMn}_{0.5}\text{Ni}_{1.5}$, $\text{ZrMn}_{0.75}\text{Ni}_{1.25}$ and $\text{ZrMn}_{1.0}\text{Ni}_{1.0}$ are the interesting compositions which can reversibly store ~ 2.2 H/F.U., ~ 3 H/F.U. and ~ 3.2 H/F.U., respectively. It is observed that $x = 1.0$ – 1.5 is a narrow range within which room temperature (and near STP) high capacity hydrides of this class can be tailored. The materials exhibit excellent thermodynamics, rapid absorption/desorption kinetics and good activation features.

Experimental techniques

All the required chemicals such as Zr, Mn and Ni were procured from Alfa Aesar Chemicals Ltd. The compositions of Zr/Mn/Ni were calculated as required for the formula $\text{ZrMn}_{2-x}\text{Ni}_x$, (where $x = 0$ – 2). The powder mixer taken in right stoichiometry was palletized by 100 KN load (pellet thickness: 5 mm and diameter: 15 mm) and the pellets were melted under inert ambient using a high frequency induction furnace (20 kW, 12 kHz) supplied by Inductotherm India pvt ltd, Ahmedabad. For hydrogen storage measurements, 2 g of samples were loaded in a metal-hydrogen high pressure reaction chamber. PCT absorption/desorption measurements have been performed by a digitalized Sievert's type apparatus. Heat of the reaction (ΔH) was calculated from the van't Hoff plots and the activation energy measurements were carried out using the standard Arrhenius relation. DSC measurements have been performed by PerkinElmer instrument and XRD analysis of all the samples were performed by Regaku mini Flex11 X-ray diffractometer employing CuK_α radiation ($\lambda = 1.541 \text{ \AA}$). XRD measurements have been performed within the 2θ range of 30° – 80° with a scanning speed of 2 s for the every 0.05° angles (step size). The lattice parameters were calculated using the unit cell refinement technique and the refined lattice constant values were compared with the standard JCPDF data source files. The crystallite

size was calculated using Scherrer method and the strain available on the crystals was calculated using the Williamson-Hall (W-H) method. Further details regarding the detailed material synthesis and processing protocols can be seen in our earlier report [17].

Results and discussion

Structural studies

Figure 1 shows the XRDs of the $\text{ZrMn}_{2-x}\text{Ni}_x$ system, x correspond to = 0, 0.5, 1.0, 1.25, 1.5 and 2, respectively. The starting phase ZrMn_2 corresponds to C14 structure and the end phase ZrNi_2 corresponds to C15 structure. The C14 structure retains up to the Mn/Ni concentration of 1.50/0.50 and any further substitution of Mn by Ni leads to its transformation to the C15 phase. Particularly, the Mn/Ni concentration range of 1.00/1.00–0.75/1.25 appears to be quite sensitive for this structural transformation. Extensive discussions are being made by researchers regarding the correlation between the phase abundance of C15 and C14 and the corresponding hydrogen storage/electrochemical performances [18–22]. In the present case, when the C15 phase abundance is dominant, the precipitation of the non-laves phase $\text{Zr}_7\text{Ni}_{10}$ alloy does also occur. Since the Mn/Ni concentration region of 0.75/1.25–0.50/1.50 brings out the non-laves phase alloy in the system (see Fig. 1), we tried to understand the effect of minor variations (of concentration within the Mn/Ni concentration region of 0.75/1.25–0.50/1.50) in its phase abundance and hydrogen storage performances and the results were communicated elsewhere.

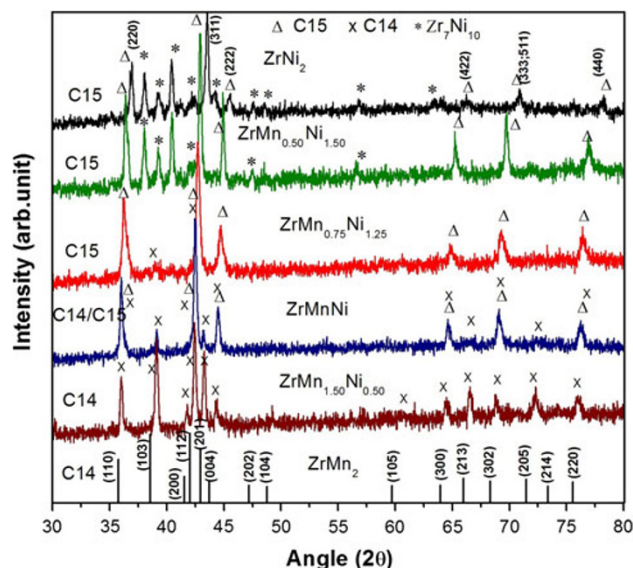


Fig. 1 XRDs of the $\text{ZrMn}_{2-x}\text{Ni}_x$ alloys ($x = 0$ – 2) prepared in the present study

As we decrease the amount of Mn in the composition, there is regular peak shifting toward the higher angle side. It shows that the lattice parameter of the system decreases with the increase of Ni content in the system. In a particular concentration (see Fig. 1), the contraction is followed by the precipitation of C15 phase also along with the C14 phase. Upon the further increase of Ni content the C14 phase gets eliminated and only C15 phase exists along with a non-laves phase of Zr_7Ni_{10} . The observed crystal structural details are summarized in the Table 1. The decrease in lattice parameters as we increase the Ni concentration can be attributed with the fact that both the covalent radius and atomic radius of Ni are smaller than that of Mn (Atomic radius of Mn and Ni are 1.79 and 1.62 Å, respectively; covalent radii of Mn and Ni are 1.17 and 1.15 Å, respectively).

The XRDs of hydrogenated $ZrMnNi$, $ZrMn_{0.75}Ni_{1.25}$ and $ZrMn_{0.5}Ni_{1.5}$ are shown in Fig. 2a, b and c. For effective comparison, the corresponding XRDs of the unhydrided samples are also given in the figure. As can be seen, the XRDs of hydrogenated samples of $ZrMnNi$ and $ZrMn_{0.75}Ni_{1.25}$ exhibit a considerable shifting toward the lower angle side. The shifting arises due to the fact that the insertion of hydrogen in the interstitial sites does lead to expansion of lattice (the upper limit of expansion is known to be one-fourth of the actual lattice parameter) [23]. The peak shifting gives us a clue that hydrides of both the materials could be stable under room temperature. However, our subsequent hydrogen liberation experiments over a range of temperatures proved that hydrogen liberation with slow kinetics is still active at room temperature itself. Thus, the presence of a small peak at the 2θ value around 42.5 (highlighted by a rectangular box) can be attributed to the existence of some portion of the material in dehydrogenated form. The other two interesting information

explored from this comparison is that (a) the phase abundance of C14 appears to increase during hydrogenation of both the $ZrMnNi$, $ZrMn_{0.75}Ni_{1.25}$ samples. It can be understood from the appearance of some dominant peaks of C14 after hydrogenation, (b) the non-laves phase Zr_7Ni_{10} which presents along with the $ZrMn_{0.75}Ni_{1.25}$ sample also gets hydrogenated and its usual orthorhombic phase itself undergoes phase transformation [24, 25]. Unlike the above two cases, in the case of $ZrMn_{0.5}Ni_{1.5}$ (Fig. 2c) the XRD of hydrogenated sample does not indicate any significant shifting from the usual XRD peak positions of its unhydrided sample. It clearly conveys us that there was no much hydrogen in the interstitial sites to cause any considerable lattice shifting. From this insight one may infer that the hydrogenated material is either not stable under room temperature or there is no hydrogenation at all. However, the subsequent experiments proved that in this case the former possibility exists (the low temperature experiments have proven that the equilibrium pressure of 1 atm occurs at temperatures lesser than room temperature).

One another noticeable behavior is that the crystallite size of these materials got reduced to a greater extent after its interaction with hydrogen (see Table 1). The reduction in the crystallite size in the case of $ZrMn_{0.5}Ni_{1.5}$ is even closer to 50 %. The crystallite size vs strain diagram for all the compositions of the present study is shown in Fig. 3. As seen in the figure, the system with higher crystallite size exhibits smaller strain and vice versa. It is also seen that the hydrided materials are incorporated with higher strain as compared to the corresponding intermetallic system.

Hydrogen storage characteristics

The hydrogen absorption kinetic curves of the as-prepared $ZrMn_{2-x}Ni_x$ alloys are shown in Fig. 4. Among all these

Table 1 The structural and microstructural details of the alloys prepared in the present study

Sr. no.	Composition	Lattice constant		Cell volume (Å) ³	Crystallite size (nm)
		a (Å)	c (Å)		
1	$ZrMn_2$ (Standard) (C14)	5.039	8.250	181.42	
2	$ZrMn_{1.5}Ni_{0.5}$ (C14)	5.001 ± 0.004	8.170 ± 0.012	176.960 ± 0.292	38.50
3	$ZrMn_{1.0}Ni_{1.0}$ (C14)	4.9921 ± 0.001	8.1458 ± 0.006	175.803 ± 0.152	41.69
	$ZrMn_{1.0}Ni_{1.0}$ (C15)	7.058 ± 0.002	7.058 ± 0.002	351.634 ± 0.225	
4	$ZrMn_{0.75}Ni_{1.25}$ (C15)	7.037 ± 0.005	7.037 ± 0.005	348.53 ± 0.711	27.82
5	$ZrMn_{0.5}Ni_{1.5}$ (C15)	7.021 ± 0.002	7.021 ± 0.002	345.92 ± 0.235	38.28
6	$ZrNi_2$ (C15)	6.902 ± 0.002	6.902 ± 0.002	328.75 ± 0.314	37.53
7	$ZrMn_{1.0}Ni_{1.0}$ (Hydride) (C15)	7.573 ± 0.004	7.573 ± 0.004	434.423 ± 0.717	28.88
	$ZrMn_{1.0}Ni_{1.0}$ (Hydride) (C14)	5.356 ± 0.003	8.728 ± 0.013	216.800 ± 0.381	
8	$ZrMn_{0.75}Ni_{1.25}$ (Hydride) (C15)	7.602 ± 0.002	7.602 ± 0.002	439.237 ± 0.315	21.73
	$ZrMn_{0.75}Ni_{1.25}$ (Hydride) (C14)	5.377 ± 0.002	8.795 ± 0.008	220.240 ± 0.238	
9	$ZrMn_{0.5}Ni_{1.5}$ (Hydride) (C15)	7.016 ± 0.002	7.016 ± 0.002	345.35 ± 0.248	30.70

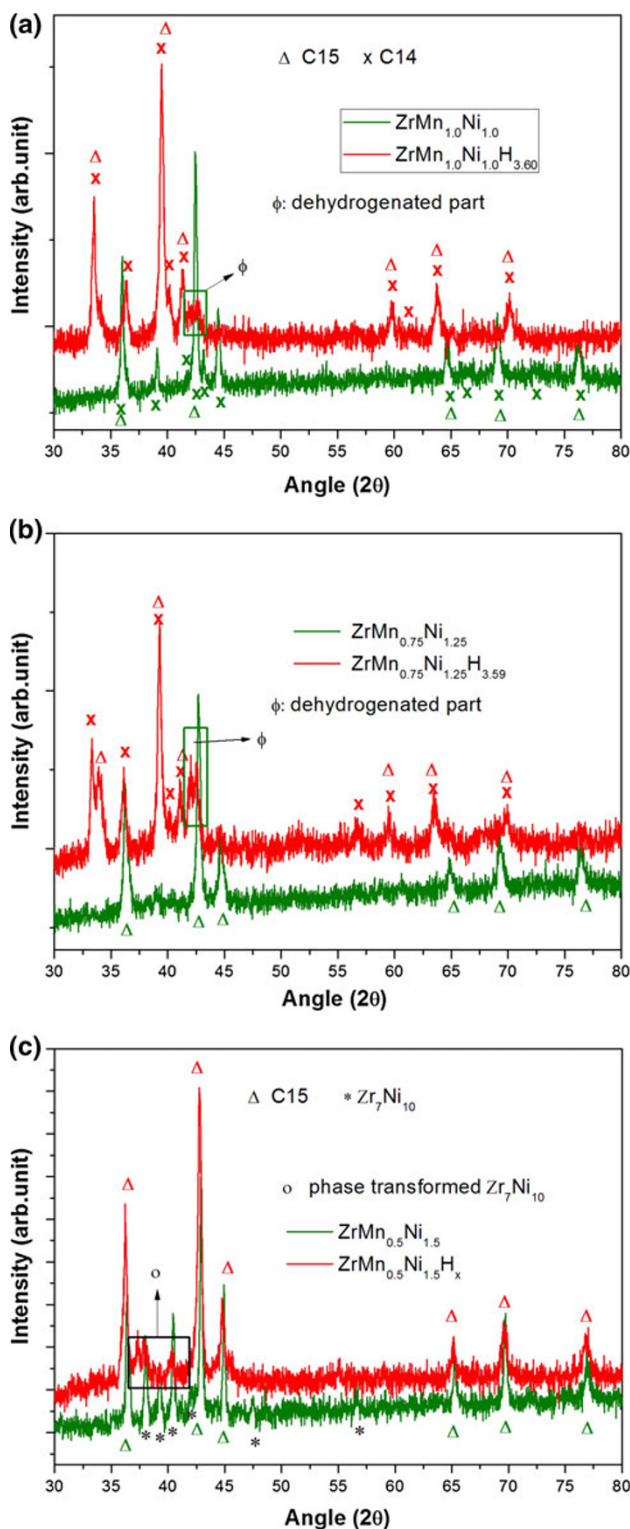


Fig. 2 Comparison of the XRDs of hydrogenated alloys, **a** ZrMnNi, **b** ZrMn_{0.75}Ni_{1.25} and **c** ZrMn_{0.5}Ni_{1.5}. XRDs of the corresponding as-received materials are also given in the figure

alloys, the ZrMn₂ alloy absorbs hydrogen with rapid kinetics when exposed to hydrogen without any activation treatments. A capacity of ~3 H/F.U. could be obtained

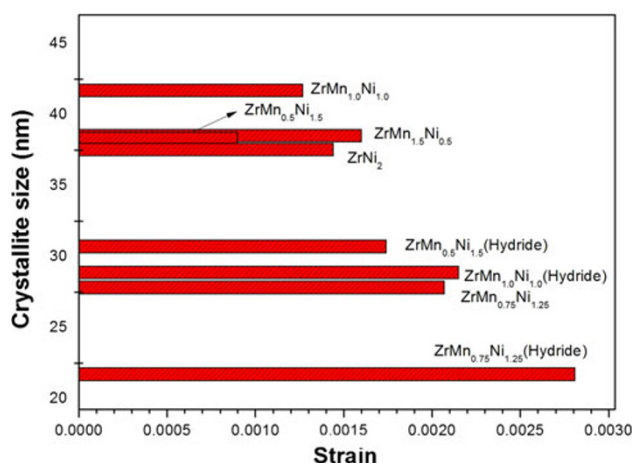


Fig. 3 The crystallite size vs strain analysis of all the alloys prepared in the present study. The hydrided materials are also given in the figure

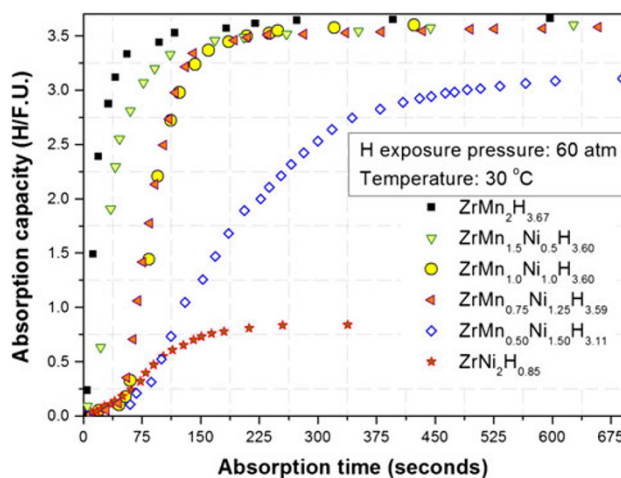


Fig. 4 The hydrogen absorption kinetics curves for all the materials prepared in the present study. The curves represent the kinetics obtained during the first time hydrogen exposure to the as-prepared samples. Hydrogenation temperature: 30 °C

within few seconds and the maximum capacity reaches 3.67 H/F.U. As we incorporate Ni in place of Mn, the absorption kinetics decreases and only little decrease in storage capacity is witnessed up to the Mn/Ni concentration of 0.75/1.25. But, when we further reduce the Mn concentration, both the absorption kinetics and storage capacity get reduced and only 0.85 H/F.U. can be stored when all the Mn is replaced by Ni. However, during hydrogen desorption, the kinetics of the Ni rich compositions are better than that of Mn rich compositions. The end materials ZrMn₂, ZrNi₂ and the intermediate composition ZrMn_{1.5}Ni_{0.5} liberate hydrogen only marginally with very poor desorption kinetics. In fact, just traceable amount of hydrogen can be observed under 100 °C and no significant improvement is observed even at ~200 °C (see Fig. 5). It

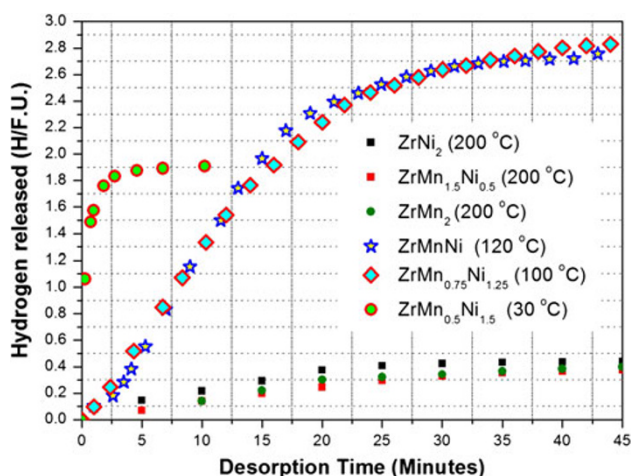


Fig. 5 The desorption kinetic curves of the hydrogenated samples. The calculated activation energy values are given in Table 2

may be due to the fact that the Mn rich compositions quickly make very stable hydrides and Ni rich composition makes only less stable or unstable hydrides. Further experiments suggested that temperature in excess of 200 °C is required for hydrogen liberation from the Mn rich phases. However, better hydrogen storage characteristics could be witnessed from some intermediate compositions such as ZrMnNi, ZrMn_{0.75}Ni_{1.25} and ZrMn_{0.5}Ni_{1.5}. These hydrides absorb and liberate hydrogen under manageable temperatures. Particularly the alloy ZrMn_{0.5}Ni_{1.5} liberates ~1.9 H/F.U. hydrogen at room temperature. The desorption activation energy values calculated for ZrMnNi, ZrMn_{0.75}Ni_{1.25} and ZrMn_{0.5}Ni_{1.5} hydrides are given in Table 2.

In the case of ZrMn_{2-x}Ni_x we noticed that the x values in the range of 1–1.5 lead to promising Zr-based AB₂ hydrides suitable for commercial applications. Our thorough investigation revealed that x in the range of 0 to <1 and 1.5 to 2 does not lead to any interesting Zr–Mn–Ni system for reversible hydrogen storage applications. The former case materials interact too strongly with hydrogen and the latter case interact poorly with hydrogen. The PCI (desorption isotherm) curves of three interesting systems within the $x = 1–1.5$ range, such as ZrMnNi, ZrMn_{0.75}Ni_{1.25} and ZrMn_{0.5}Ni_{1.5} are shown in Fig. 6a, b and c, respectively. From the nature of the PCT desorption curves

obtained in these compositions it is clearly understood that any little changes made in the Mn concentration within this small x value range lead to big changes in the thermodynamics of the system. Our estimation reveals that ZrMnNi restores ~3.2 H/F.U. and works within the temperature range of 120–180 °C, ZrMn_{0.75}Ni_{1.25} restores ~3 H/F.U. and works well within the temperature range of 60–140 °C and ZrMn_{0.5}Ni_{1.5} restores ~2.1 H/F.U. and works well within the temperature range of 10–60 °C. One can understand from the PCT curves that, when we decrease the concentration of Mn = 1 to Mn = 0.5, the stability of the hydride phase gets dramatically reduced and the plateau pressure varies significantly with respect to temperature. The van't Hoff plots for the said three compositions such as ZrMnNi, ZrMn_{0.75}Ni_{1.25} and ZrMn_{0.5}Ni_{1.5} are shown in Fig. 7 and the calculated thermodynamic data are given in Table 2. The equilibrium pressure of 1 atm in these three systems can be obtained at the temperatures of 120, 100 and –20 °C, respectively. The van't Hoff plots also prove that thermodynamics of the system varies considerably within a narrow range of Mn concentration, i.e. 0.75–1.5. Such behavior can strike considerable applications for heat storage and electrochemical devices. Further, the van't Hoff diagram clearly indicates that all these three system covers the working range of the commercial hydrogen fuel cells.

The PCT (re)absorption isotherm of the composition ZrMnNi, ZrMn_{0.75}Ni_{1.25} and ZrMn_{0.5}Ni_{1.5} are given in Fig. 8a. The composition ZrMn_{0.5}Ni_{1.5} exhibits much higher plateau pressure as compared to ZrMn_{0.75}Ni_{1.25} and ZrMn_{0.5}Ni_{1.5}. It clearly shows the large differences in their thermodynamic features between the x values of 1.25–1.5 in the ZrMn_{2-x}Ni_x system. The reversible hydrogen absorption kinetic plots for the systems such as ZrMnNi, ZrMn_{0.75}Ni_{1.25} and ZrMn_{0.5}Ni_{1.5} are shown in Fig. 8b. As seen, ZrMnNi system restores hydrogen in excess of 3 H/F.U. and nearly half of this capacity is absorbed within 5 s. ZrMn_{0.75}Ni_{1.25} also stores almost the similar capacity but ZrMn_{0.5}Ni_{1.5} stores only 2.2 H/F.U. However, it should also be noted that unlike ZrMnNi and ZrMn_{0.75}Ni_{1.25}, ZrMn_{0.5}Ni_{1.5} can absorb and release this capacity under room temperature. The DSC curves of all the ZrMn_{2-x}Ni_x system are shown in Fig. 9. The DSC curves also confirm that the ZrMn_{0.5}Ni_{1.5} sample behaves much differently as

Table 2 Summary of the observed heat of desorption and activation energy values

Sr. no.	Composition	$-\Delta H$ (kJ/mol H)	ΔS (J/(K mol H))	Desorption temp. at equilibrium pressure of 0.1 MPa	Activation energy (kJ/mol)	Effective H capacity (H/F.U.)
1	ZrMn _{1.0} Ni _{1.0}	32.14 ± 1.52	81.43 ± 3.45	119.10	21.03 ± 0.22	3.3
2	ZrMn _{0.75} Ni _{1.25}	27.97 ± 1.82	74.87 ± 4.32	100.01	17.91 ± 0.67	3.0
3	ZrMn _{0.5} Ni _{1.5}	18.61 ± 1.14	73.74 ± 3.60	–20.30	13.21 ± 0.16	2.2

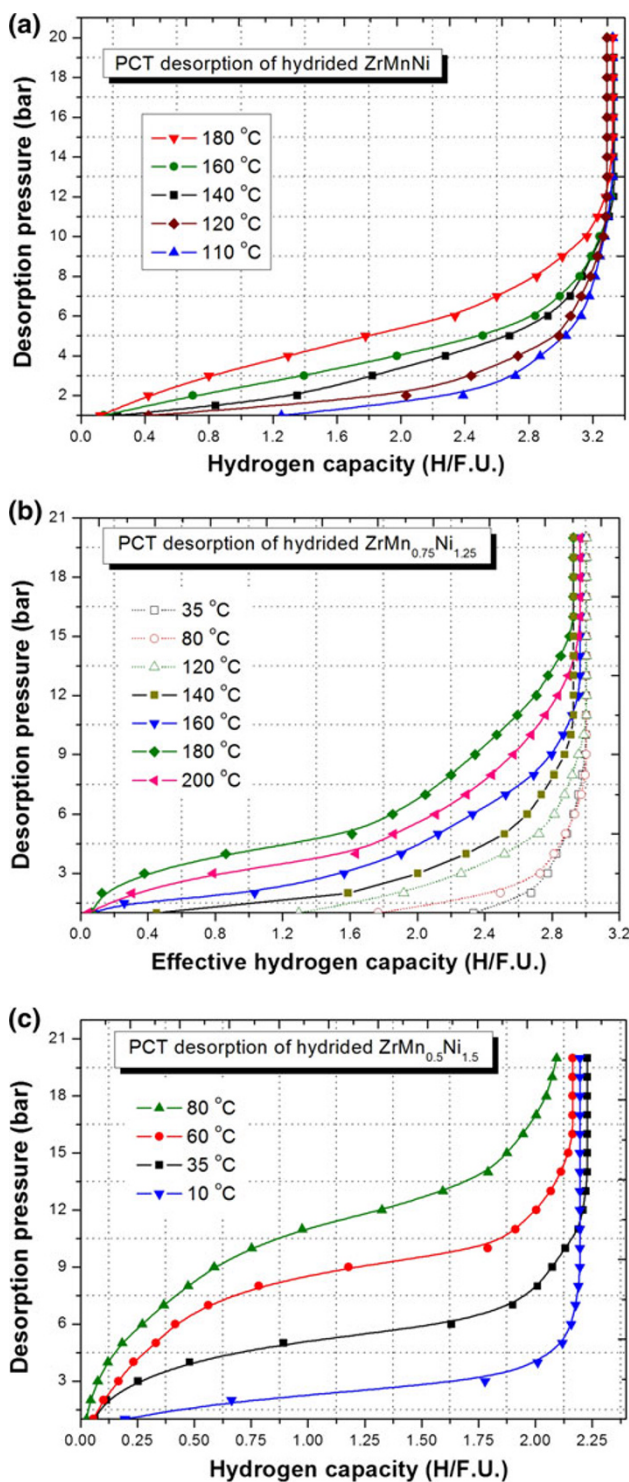


Fig. 6 a, b, c The PCT desorption isotherms of the alloys. **a** ZrMnNi, **b** ZrMn_{0.75}Ni_{1.25} and **c** ZrMn_{0.5}Ni_{1.5}

compared to all other compositions. This curious observation in the case of ZrMn_{0.5}Ni_{1.5} may be related with the heat transfer associated with the evolution of residual hydrogen so as to transform as hydrogen free metal phase. Because, only in the case of ZrMn_{0.5}Ni_{1.5} does the

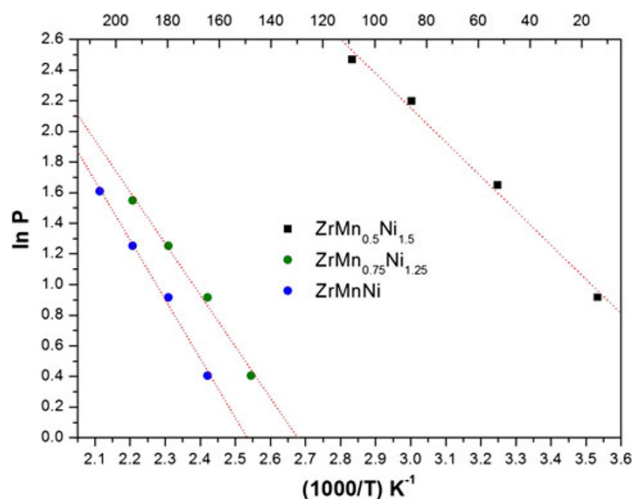


Fig. 7 The van't Hoff plots (dehydrogenation) for the compositions such as ZrMnNi, ZrMn_{0.75}Ni_{1.25} and ZrMn_{0.5}Ni_{1.5}

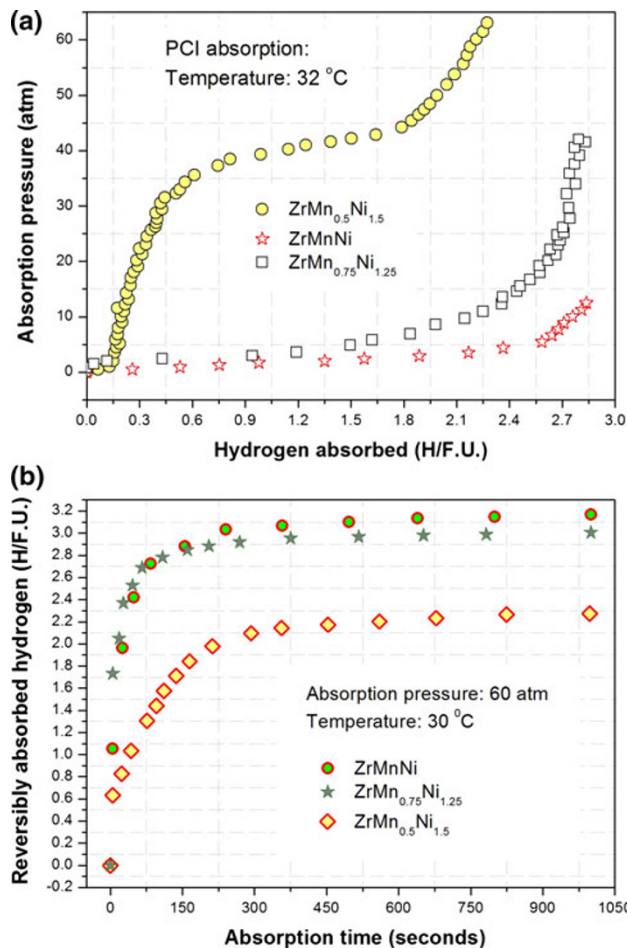


Fig. 8 **a** The PCT isotherms for reversible hydrogen absorption for ZrMnNi, ZrMn_{0.75}Ni_{1.25} and ZrMn_{0.5}Ni_{1.5} and **b** the reversible hydrogen absorption kinetics of ZrMnNi, ZrMn_{0.75}Ni_{1.25} and ZrMn_{0.5}Ni_{1.5} alloys

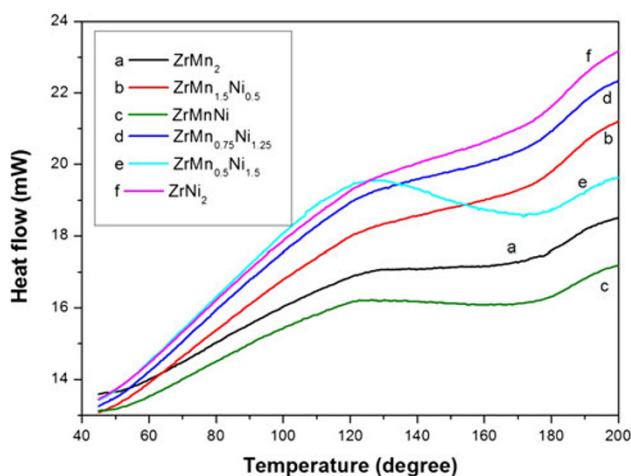


Fig. 9 DSC curves of hydrided $ZrMn_{2-x}Ni_x$ alloys ($x = 0-2$)

hydrogen liberation become effective at lower temperatures. Note that $ZrNi_2$ do not possess considerable hydrogen above room temperature and any composition above Ni/Mn concentration of 0.5/1.5 release only very small amount of hydrogen at the temperatures less than 200 °C (also refer desorption PCTs). Thus, the DSC profile of all other samples except $ZrMn_{0.5}Ni_{1.5}$ looks as similar as each other. The hydrogen absorption/desorption behavior of $ZrMn_{2-x}Ni_x$ for $x = 1-1.5$ makes it clear that these materials are suitable for variety of stationary applications (as for example, large stationary hydrogen storage cylinders in hydrogen production/distribution spots, H isotope stores etc.) and even mobile applications. Particularly, in the case of $ZrMn_{0.75}Ni_{1.25}$, the reversible hydrogen storage of ~ 2 H/F.U. within few seconds shows that these are candidates par excellence for device applications.

In the present Zr–Mn–Ni alloy system, the hydrogen capacity of C14 phase is, in general, higher than the capacity of C15 phase, which is contrary to the observation of some earlier reports [21, 26, 27]. However, from performance point of view, particularly for low temperature desorption, C15 phase co-existing with the non-laves phase of Zr_7Ni_{10} is found to be better. Song et al. [28, 29] have earlier studied the $ZrMn_{0.9-x}V_xNi_{1.1}$ (x from 0.1 to 0.8) system and concluded that C15 phase with higher stacking faults performs better for electrochemical applications. In the present case, since Zr_7Ni_{10} concurrently presents with the C15 phase, the higher sorption performances cannot be solely related to the stacking faults itself. Moreover, there are reports suggesting that the Zr_7Ni_{10} offers catalytic activity for surface reactions and also acts as a medium for charge diffusion [30–33]. However, in spite of the presence of Zr_7Ni_{10} phase since few C15 compositions did not store hydrogen appreciably, it appears to be the distinct electronic structure of some composition of Zr–Mn–Ni makes

the difference. Particularly, any compositions within the $ZrMn_{0.75}Ni_{1.25}$ and $ZrMn_{0.50}Ni_{1.50}$ could be promising.

Conclusions

In the case of $ZrMn_{2-x}Ni_x$ laves phase system, thermodynamically promising hydrogen storage alloys can be made within the range of $1.5 \leq x \leq 1$. $ZrMn_2$ and $ZrMn_{1.5}Ni_{0.5}$ absorb ~ 3.6 H/F.U., but the absorbed hydrogen cannot be liberated under manageable conditions. $ZrMnNi$, $ZrMn_{0.75}Ni_{1.25}$ and $ZrMn_{0.5}Ni_{1.5}$ hydrides reversibly store hydrogen capacity such as 3.2 H/F.U., 3 H/F.U. and 2.2 H/F.U., respectively. Each of these hydrides stores at least half of its effective capacity within 1 min of charging time. The working range of $ZrMnNi$, $ZrMn_{0.75}Ni_{1.25}$ and $ZrMn_{0.5}Ni_{1.5}$ are 120–180 °C, 60–120 °C and 10–60 °C, respectively. Interesting thermodynamic behavior could be witnessed when we proceed from $ZrMn_{0.75}Ni_{1.25}$ to $ZrMn_{0.5}Ni_{1.5}$ system which is also confirmed by DSC analysis.

Acknowledgments The authors thank Dr. V.C. Shahni of BARC for discussions. Dr. H.K. Singh and Dr. V.P.S. Awana of NPL are thanked for providing XRD facility. D.P.S thanks UGC, India for D.S. Kothari post doctoral fellowship and V.K thanks Dept. of Atomic Energy, India for Senior Research Fellowship. This work has been carried out under the financial assistance provided by BRNS, Department of Atomic Energy, India.

Open Access This article is distributed under the terms of the Creative Commons Attribution License which permits any use, distribution, and reproduction in any medium, provided the original author(s) and the source are credited.

References

- Fujii, H., Saga, M., Okamoto, T.: Magnetic, crystallographic and hydrogen absorption properties of YMn_2 and $ZrMn_2$ hydrides. *J. Less Common Met.* **130**, 25–31 (1987)
- Fujitani, S., Yonezu, I., Saito, T., Furukawa, N., Akiba, E., Hayakawa, H., Ono, S.: Relation between equilibrium hydrogen pressure and lattice parameters in pseudobinary Zr–Mn alloy systems. *J. Less Common Met.* **172–174**, 220–230 (1991)
- Young, K., Fetcenko, M.A., Koch, J., Morii, K., Shimizu, T.: Studies of Sn, Co., Al, and Fe additives in C14/C15 Laves alloys for NiMH battery application by orthogonal arrays. *J. Alloys Compd.* **486**, 559–569 (2009)
- Matsumura, T., Yukawa, H., Morinaga, M.: Alloying effects on the electronic structure of $ZrMn_2$ intermetallic hydride. *J. Alloys Compd.* **279**, 192–200 (1998)
- Gesari, S.B., Pronsato, M.E., Visintin, A., Juan, A.: Hydrogen Storage in AB₂ Laves Phase (A = Zr, Ti; B = Ni, Mn, Cr, V): binding energy and electronic structure. *J. Phys. Chem. C.* **114**, 16832–16836 (2010)
- Matsumura, T., Yukawa, H., Morinaga, M.: Alloying effects on the electronic structure of $ZrMn_2$ intermetallic hydride. *J. Alloys Compd.* **279**(2), 192–200 (1998)
- Du, Y.L., Yang, X.G., Lei, Y.Q., Zhang, M.S.: Hydrogen storage properties of $Zr_{0.8}Ti_{0.2}(Ni_{0.6}Mn_{0.3-x}V_{0.1+x}Cr_{0.05})_2$ ($x = 0.0$,

- 0.05, 0.15, 0.2) alloys. *Int. J. Hydrogen Energy* **27**, 695–697 (2002)
8. Pontonnier, L., Miraglia, S., Fruchart, D., Soubeyroux, J.L., Baudry, A., Boyer, P.: Structural study of hyperstoichiometric alloys $ZrMn^{2+x}$ and their hydrides. *J. Alloys Compd.* **186**, 241–248 (1992)
 9. Lee, S.M., Lee, H., Kim, J.H., Lee, P.S., Lee, J.Y.: A study on the development of hypo-stoichiometric Zr-based hydrogen storage alloys with ultra-high capacity for anode material of Ni/MH secondary battery. *J. Alloys Compd.* **308**, 259–268 (2000)
 10. Sun, J.C., Li, S., Ji, S.J.: The effects of the substitution of Ti and La for Zr in $ZrMn_{0.7}V_{0.2}Co_{0.1}Ni_{1.2}$ hydrogen storage alloys on the phase structure and electrochemical properties. *J. Alloys Compd.* **446–447**, 630–634 (2007)
 11. Bendersky, L.A., Wang, K., Levin, I., Newbury, D., Young, K., Chao, B., Creuziger, A.: $Ti_{1.25}Zr_{2.1}V_{1.0}Cr_{8.5}Mn_xCo_{1.5}Ni_{46.5-x}$ AB₂-type metal hydride alloys for electrochemical storage application. *J. Power Sources* **218**, 474–486 (2012)
 12. Jong-Man, P., Jai-Young, L.: Hydrogenation characteristics of the $Zr_{1-x}Ti_xCr_{1-y}Fe_{1+y}$ laves phase alloys. *J. Less Common Metals.* **160**(2), 259–271 (1990)
 13. Yasuoka, S., Magari, Y., Murata, T., Tanaka, T., Ishida, J., Nakamura, H., Nohma, T., Kahara, M., Baba, Y., Teraoka, H.: Development of high-capacity nickel-metal hydride batteries using superlattice hydrogen-absorbing alloys. *J. Power Sources* **156**, 662–666 (2006)
 14. Xiaoguang, Y., Yonquan, L., Jing, W., Qidong, W.: The electrochemical performances of Zr based hydrogen storage alloys. *Trans. NFsoc.* **5**, 61–65 (1995)
 15. Suzuki, A., Nishimiya, N.: Thermodynamic properties of $Zr(Ni_xMn_{1-x})_2-H_2$ systems. *Mat. Res. Bull.* **9**, 1559–1571 (1984)
 16. Kim, D.M., Lee, S.M., Jang, K.J., Lee, J.Y.: The electrode characteristics of over-stoichiometric $ZrMn_{0.5}V_{0.5}Ni_{1.4+y}$ ($y = 0.0, 0.2, 0.4$ and 0.6) alloys with C15 Laves phase structure. *J. Alloys Compd.* **268**(1–2), 241–247 (1998)
 17. Kumar, V., Pukazhselvan, D., Singh, S.K.: Hydrogen Storage Characteristics of $MnNi_{5-x}M_x$ ($M = Cu, Mn$ and Al). *Adv. Sci. Lett.* **18**, 164–169 (2012)
 18. Du, Y.L., Yang, X.G., Zhang, Q.A., Lei, Y.Q., Zhang, M.S.: Phase structures and electrochemical properties of the Laves phase hydrogen storage alloys $Zr_{1-x}Ti_x(Ni_{0.6}Mn_{0.3}V_{0.1}Cr_{0.05})_2$. *Int. J. Hydrogen Energy.* **26**(4), 333–337 (2001)
 19. Young, K., Ouchi, T., Huang, B., Chao, B., Fetcenko, M.A., Bendersky, L.A., Wang, K., Chiu, C.: The correlation of C14/C15 phase abundance and electrochemical properties in the AB₂ alloys. *J. Alloys Compd.* **506**(2), 841–848 (2010)
 20. Young, K., Nei, J., Ouchi, T., Fetcenko, M.A.: Phase abundances in AB₂ metal hydride alloys and their correlations to various properties. *J. Alloys Compd.* **509**(5), 2277–2284 (2011)
 21. Huot, J., Akiba, E., Ogura, T., Ishido, Y.: Crystal structure, phase abundance and electrode performance of Laves phase compounds $(Zr, A)V_{0.5}Ni_{1.1}Mn_{0.2}Fe_{0.2}$ ($A = Ti, Nb$ or Hf). *J. Alloys Compd.* **218**(1), 101–109 (1995)
 22. Song, X.Y., Zhang, X.B., Lei, Y.Q., Zhang, Z., Wang, Q.D.: Effect of microstructure on the properties of Zr–Mn–V–Ni AB₂ type hydride electrode alloys. *Int. J. Hydrogen Energy* **24**(5), 455–459 (1999)
 23. Figiel, H., Osuchowski, S., Paja, A.: Unit cell expansion in Laves phase-type compounds caused by interstitial hydrogen. *Phys. Stat. Sol. (a)* **204**, 3286–3290 (2007)
 24. Takeshita, H.T., Fujiwara, N., Oishi, T., Noréus, D., Takeichi, N., Kuriyama, N.: Another unusual phenomenon for Zr_7Ni_{10} : structural change in hydrogen solid solution and its conditions. *J. Alloys Compd.* **360**, 250–255 (2003)
 25. Takeshita, H.T., Kondo, S., Miyamura, H., Takeichi, N., Kuriyama, N., Oishi, T.: Re-examination of Zr_7Ni_{10} single-phase region. *J. Alloys Compd.* **376**, 268–274 (2004)
 26. Zhang, Q.A., Lei, Y.Q., Yang, X.G., Ren, K., Wang, Q.D.: Annealing treatment of AB₂-type hydrogen storage alloys: II Electrochemical properties. *J. Alloys Compd.* **292**, 241–246 (1999)
 27. Du, Y.L., Yang, X.G., Zhang, Q.A., Leo, Y.Q., Zhang, M.S.: Phase structures and electrochemical properties of the Laves phase hydrogen storage alloys $Zr_{1-x}Ti_x(Ni_{0.6}Mn_{0.3}V_{0.1}Cr_{0.05})_2$. *Int. J. Hydrogen Energy* **26**, 333–337 (2001)
 28. Song, X., Zhang, X., Lei, Y., Zhang, Z., Wang, Q.: Effect of microstructure on the properties of Zr–Mn–V–Ni AB₂ type hydride electrode alloys. *Int. J. Hydrogen Energy* **24**, 455–459 (1999)
 29. Yang, X.G., Zhang, W.K., Lei, Y.Q., Wang, Q.D.: Electrochemical properties of Zr–V–Ni system hydrogen storage alloys. *J. Electrochem. Soc.* **146**, 1245–1250 (1999)
 30. Ruiz, F.C., Castro, E.B., Real, S.G., Peretti, H.A., Visintin, A., Triaca, W.E.: Electrochemical characterization of AB₂ alloys used for negative electrodes in Ni/MH batteries. *Int. J. Hydrogen Energy* **33**, 3576–3580 (2008)
 31. Visintin, A., Peretti, H.A., Ruiz, F., Corso, H.L., Triaca, W.E.: Effect of additional catalytic phases imposed by sintering on the hydrogen absorption behavior of AB₂ type Zr-based alloys. *J. Alloys Compd.* **428**, 244–251 (2007)
 32. Ruiz, F.C., Castro, E.B., Peretti, H.A., Visintin, A.: Study of the different Zr_xNi_y phases of Zr-based AB₂ materials. *Int. J. Hydrogen Energy* **35**, 9879–9887 (2010)
 33. Bendersky, L.A., Wang, K., Boettinger, W.J., Newbury, D.E., Young, K., Chao, B.: Examination of multiphase (Zr, Ti)(V, Cr, Mn, Ni)₂ Ni-MH electrode alloys: part II solid-state transformation of the interdendritic B₂ phase. *Metall. Mater. Trans. A* **41**, 1891–1906 (2010)